ACADÉMIE
DES SCIENCES
INSTITUT DE FRANCE

Comptes Rendus
Chimie

Mohammed Javeed Siddique and Punitha Kumar Akhas

Advancing energy efficiency: thermomechanical characterization of plastic-infused concrete for sustainable building solutions

Volume 27, Special Issue S3 (2024), p. 29-43

Online since: 22 November 2024

Part of Special Issue: Materials and Energy Valorization of Biomass and Waste: The Path for Sustainability and Circular Economy Promotion

Guest editors: Mejdi Jeguirim (Université de Haute-Alsace, Institut de Sciences des Matériaux de Mulhouse, France) and Salah Jellali (Sultan Qaboos University, Oman)

https://doi.org/10.5802/crchim.330

The Comptes Rendus. Chimie *are a member of the Mersenne Center for open scientific publishing*
www.centre-mersenne.org — e-ISSN : 1878-1543

ACADÉMIE DES SCIENCES
INSTITUT DE FRANCE

Comptes Rendus. Chimie
2024, Vol. 27, Special issue S3, p. 29-43
https://doi.org/10.5802/crchim.330

Research article

Materials and Energy Valorization of Biomass and Waste: The Path for Sustainability and Circular Economy Promotion

Advancing energy efficiency: thermomechanical characterization of plastic-infused concrete for sustainable building solutions

Mohammed Javeed Siddique [a, b] **and Punitha Kumar Akhas** [*, a]

[a] School of Civil Engineering, Vellore Institute of Technology, Vellore, India

[b] Civil and Environmental Engineering Department, A'Sharqiyah University, Ibra, Oman

E-mails: mohammed.javeed@asu.edu.om (M. J.Siddique), punithakumar.a@vit.ac.in (A. Punitha Kumar)

Abstract. Global energy demands within buildings are escalating, driven by increased dependence on energy-intensive systems such as air conditioning. This surge necessitates innovative solutions to reduce energy consumption and promote sustainability in construction practices. Simultaneously, the persistent problem of plastic waste presents an environmental challenge, with recycling efforts lagging behind the rapidly growing volumes of discarded materials. This study addresses both issues by investigating the feasibility of using recycled plastic materials—low-density polyethylene (LDPE), polypropylene (PP), polyester, and high-density polyethylene (HDPE)—as partial sand substitutes in concrete for roofing applications. The objectives of this research include reducing air conditioning costs, decreasing carbon emissions, and shortening the payback period for energy-efficient building practices. Specifically, buildings situated in the hot–dry climate of Muscat, Oman, and the composite climate of New Delhi, India, were studied. The evaluation of the modified concrete's mechanical and thermophysical properties indicates that the incorporation of 30 wt% LDPE yields the most significant economic and environmental benefits. This modification leads to the highest annual savings, calculated at 0.9946 $/m² in Muscat and 0.9928 $/m² in New Delhi, along with a marked reduction in carbon emissions—19 kg/kWh in Oman and 18.2 kg/kWh in New Delhi. Additionally, the use of 10 wt% HDPE results in the fastest payback, recorded at 1.37 years.

Keywords. Sustainable building materials, HVAC energy load, Carbon mitigation, Waste plastics in construction, Hot–dry and composite climates.

Manuscript received 24 February 2024, revised 10 May 2024 and 3 July 2024, accepted 26 August 2024.

1. Introduction

The phenomena of urbanization and increasing populations are two pivotal factors shaping the contemporary world. Earth's clay and sand serve as essential raw materials in the construction industry; however, their extensive use may result in the depletion of vital resources. Consequently, researchers are increasingly motivated to explore both innovative materials and recycling strategies for waste generated across various industries [1]. Plastics are ubiquitously present in the modern world, and their degradation, particularly in materials like polypropylene

* Corresponding author

(PP), polycarbonate, and PVC, can take up to 500 years [2]. The Environmental Protection Agency estimates that only approximately 7% of plastic waste is currently recycled annually [3]. Utilizing plastics in brick production not only mitigates plastic pollution but also yields both environmental and economic benefits [4]. India and China are dominant forces in the brick manufacturing industry, with their combined annual production surpassing 240 billion bricks [5]. The traditional approach to brick manufacturing, reliant predominantly on sand and cement, significantly contributes to carbon emissions and depletes crucial natural resources [6]. In contrast, the incorporation of plastic materials into brick production is gaining recognition as a sustainable and eco-friendly alternative in civil engineering [7]. A study was conducted that employed glass powder and PP particles in the manufacture of fired clay bricks. The results indicated that bricks incorporating waste glass demonstrated superior mechanical properties, as evidenced by compression tests when compared to bricks utilizing plastic waste [8]. Plastic, a material with both detrimental and beneficial attributes, poses challenges to long-term sustainability efforts due to its resistance to biodegradation. In light of this, studies have investigated the use of thermoplastic materials such as high-density polyethylene (HDPE) and PP for fabricating bricks through physical recycling techniques. One such study showed that bricks made from HDPE displayed a compressive strength of 11.19 N/mm^2, exceeding the 10.5 N/mm^2 strength found in high-quality traditional bricks [9]. Further research has broadened the scope to include the utilization of plastic waste and other thermoplastic materials in construction applications. For example, Balasubramanian et al. examined the effects of replacing electronic waste in concrete at various proportions (10%, 20%, and 30%), concluding that a 20% replacement yielded optimal results [10]. Similarly, Muthu et al. found that the maximum compressive strength achieved for blocks made from e-waste plastic was 20.48 N/mm^2, outperforming both sand-based and fly-ash blocks [11]. Few researchers have concentrated on evaluating the impact of both polymer and nonpolymer admixtures on concrete roofing. These studies primarily examine the prospective advantages of minimizing air conditioning costs and mitigating carbon emissions [12]. Ibrahim et al. employed polyethylene terephthalate (PET) as a partial replacement for sand in a series of six concrete mixtures, with substitution ratios ranging from 0% to 50%. The experimental results showed that the inclusion of a sand substitute influenced the mechanical properties of the building materials at varying levels [13]. The research by Pratap et al. demonstrated that substituting 3% of sand with waste PET led to an optimal compressive strength of 36.66 N/mm^2, surpassing that of conventional mixtures [14]. Similarly, Prashanth et al. incorporated burned solid waste and recycled plastic waste as alternative materials in concrete, proving its practicality in creating more cost-effective construction materials and significantly reducing building costs [15]. Vivek et al. conducted an extensive study to explore the properties of concrete blocks made with a partial replacement of fine aggregate using low-density polyethylene (LDPE). The outcomes of this study suggest that the integration of plastic elements not only aids in conserving invaluable natural resources but also acts as an effective strategy in mitigating the proliferation of plastic waste in the environment [16]. In a similar vein, Ali et al. undertook research on the recycling of polyethylene and PP waste, targeting the production of plastic blocks. Their findings indicate that the use of recycled plastic waste as a cement substitute in the production of plastic-reinforced blocks provides a viable and green, eco-friendly alternative [17]. This approach not only mitigates the accumulation of plastic waste but also yields sustainable and economically viable building materials. Idrees et al. focused on the integration of eco-friendly methodologies in the fabrication of low shrinkage fired clay blocks, achieved through the incorporation of recycled plastic dust as a primary component. The studies indicated that the compressive strength decreased as the proportion of recycled plastic dust increased [18]. Such an approach confers advantages like reducing the consumption of natural soil resources and enabling the production of bricks with improved weight and volumetric stability. Arya et al. investigated the replacement of conventional fine aggregates with a blend of e-waste, specifically keyboards, and other discarded materials such as eggshells, fly ash, and silica fumes. Preliminary results indicate that these alternative materials show promise in both mitigating environmental impact and enhancing sustainable construction practices [19]. Modifications in the

mechanical and functional attributes of concrete pavement blocks were observed when sand was substituted with plastic; a 4% replacement of sand by plastic led to an improvement in compressive strength. However, as the proportion of plastic increased, a corresponding decline in structural integrity was noted [20]. Haque et al. conducted a study focusing on the use of recycled PET plastic bottles in the fabrication of bricks [21]. The prevailing literature largely emphasizes the critical examination of compressive strength while also considering factors such as reducing cooling expenses, lowering carbon emissions, and evaluating the significance of the payback period (PBP) [22]. A few studies have delved into the thermal transmission characteristics of insulation materials in construction, finding that smaller surface factors in these materials result in a slower response to short-wave radiation, while larger surface factors lead to time delays [23]. Saboor et al. primarily examined the conversion of waste materials such as rice husk, sawdust, coir pith, and fly ash into viable construction materials. Their findings revealed that walls constructed from rice husk mud bricks offer the highest reduction in air conditioning costs, amounting to 1.74 $\$/m^2$, along with an acceptable PBP of 1.17 years and higher annual carbon emission mitigation values of 33.35 kg/kWh [24]. Few studies have focused on challenges associated with moisture-induced damage such as rutting resistance absorption [25] and wetness sensitivity [26]. A study on obsidian mortar, using waste brick powder and reinforced with PP fibers, demonstrated that criteria for rutting resistance and wetness sensitivity were satisfied at a temperature of 25 °C [27].

An extensive review of the existing literature highlights a significant gap in research on the use of plastic waste to improve the structural and thermal properties of concrete roofing. This gap extends to the potential of these materials to reduce air conditioning costs and shorten the PBP for buildings. This study employs an innovative approach by leveraging the dynamic thermal properties of building materials to decrease energy consumption associated with air conditioning. It investigates the cost-saving benefits of concrete samples incorporating various types of plastics such as LDPE, PP, HDPE, and polyester. The research also assesses the reduction in carbon emissions and determines the PBPs for the modified concrete samples. This investigation contributes to the development of environmentally sustainable building materials by integrating recycled plastics into concrete.

2. Materials and methods

2.1. *Materials*

The production of concrete samples involves mixing fine aggregate, coarse aggregate, cement, and water. The inclusion of recycled plastic scraps is anticipated to enhance the thermal properties of the resultant material, based on observations made during this study. Utilizing concrete that incorporates waste plastics is economically viable as it reduces the demand for virgin resources, which can be costly to produce and transport. In this study, four types of plastic materials—LDPE, HDPE, PP, and polyester—are considered as potential substitutes for sand in the mix. Figure 1 illustrates the plastic materials used. Ordinary Portland cement of grade 53 was utilized in accordance with IS 12269: 2013. The mix design for M30-grade concrete was formulated following the guidelines set forth in IS 10262. Subsequently, three distinct concrete specimens for each type of plastic were prepared (Figure 2); the specimens had dimensions of 100 × 100 × 100 mm. After a 24 h setting period, the samples were carefully demolded to maintain their structural integrity. These specimens then underwent a rigorous 28 day water-curing phase. The roofing concrete generally consists of a 0.15 m thick reinforced cement concrete covered with 0.015 m of cement plaster on both its top and bottom surfaces.

Tables 1 and 2 furnish detailed information on the physical and chemical composition of the cement. Crushed aggregate with a particle size of 20 mm was used for the concrete casting, meeting the specifications set forth in IS 383. The aggregate has a density of 2.78 g/cm^3, a water absorption rate of 0.83%, and a fineness modulus of 7.22. Density was ascertained by measuring the mass and volume of the material [28]. The fine aggregate used comprises natural river sand with a maximum particle size of 2.36 mm. The specified plastic materials—LDPE, PP, polyester, and HDPE—are integrated into the concrete samples at varying percentages of 10, 20, and 30, substituting sand to investigate their thermophysical

Figure 1. (a) Low-density polyethylene, (b) high-density polyethylene, (c) polypropylene, and (d) polyester.

Figure 2. Preparation of concrete samples.

Table 1. Percentage oxide composition of cement

Composition	%
SiO_2	20.72
Al_2O_3	4.88
Fe_2O_3	2.95
CaO	61.83
MgO	1.39
Na_2O	0.19
K_2O	0.67
SO_3	2.33
LOI	3.17

Table 2. Properties of cement

Material	Color	Blaine fineness	Density
Cement	Gray	351 m^2/kg	3.15 g/cm^3

properties. These plastic materials are reduced to a finely sized, rounded powder form with an average particle size ranging from 0.7 to 1 mm, using a pulverizer. Two distinct climatic zones, Muscat and New Delhi, were selected based on the American Society of Heating, Refrigerating and Air-Conditioning Engineers (ASHRAE) meteorological data [29]. Thermoeconomic analysis was conducted, focusing on key parameters such as annual savings in air conditioning and electricity expenses, cost benefits over time, PBPs, and carbon emission reduction [30]. Figure 3 displays the monthly degree-hours for cooling and heating in both Muscat and New Delhi. Thermophysical properties of the modified concrete samples were then measured at room temperature.

2.2. *Analytical method*

The admittance method is utilized to compute transient thermal transmittance using matrix algebra, as described in the Chartered Institution of Building Services Engineers guide (CIBSE, 2006). Mathematical calculations for concrete roofing materials were performed, ensuring that the program variance remains below 1% [31,32]. The heat transfer properties were analyzed using the one-dimensional heat diffusion equation to determine their effectiveness in various concrete compositions:

$$\frac{\partial^2 T}{\partial V^2} = \frac{1}{\alpha}\frac{\partial T}{\partial \tau} \tag{1}$$

The boundary condition at the roof's inner surface:

$$\left(\frac{\partial T}{\partial V}\right)_{V=0} = h_{\mathrm{i}}[T_{V=0}(\tau) - T_{\mathrm{i}}] \tag{2}$$

The boundary condition at the roof's outer surface:

$$\left(\frac{\partial T}{\partial V}\right)_{V=L} = h_{\mathrm{o}}[T_{\mathrm{s}}(\tau) - T_{V=L}(\tau)] \tag{3}$$

Here, $T_{V=0}$ represents the inner surface temperature of the roof/wall, $T_{V=L}$ represents the outer surface temperature of the roof/wall, T_{i} is the indoor temperature, and T_{s} is the sol-air temperature. According to CIBSE guidelines, the internal and external heat transfer coefficients for roofs are 10 and 25 $W{\cdot}m^{-2}{\cdot}K^{-1}$, respectively.

$$T = [M\sinh(Vl + \mathrm{j}Vl) + N\cosh(Vl + \mathrm{j}Vl)] \times \exp(\mathrm{j}2\pi\tau/P) \tag{4}$$

where $V = \sqrt{\pi\rho c_p/ks}$
p = period
l = finite thickness
M = heat flux
N = thermal resistance.

$$\begin{bmatrix} T_{\mathrm{i}} \\ q_{\mathrm{i}} \end{bmatrix} = \begin{bmatrix} \cosh(c+\mathrm{j}c) & (\sinh(c+\mathrm{j}c))/b \\ b\sinh(c+\mathrm{j}c) & \cosh(c+\mathrm{j}c) \end{bmatrix} \begin{bmatrix} T_{\mathrm{o}} \\ q_{\mathrm{o}} \end{bmatrix} \tag{5}$$

where cyclic thickness $(c) = Vl$
T = periodic temperature
q = periodic heat flux
slab admittance $(b) = \sqrt{\mathrm{j}2\pi k\rho c_p/s}$.

$$\begin{bmatrix} r_1 & r_2 \\ r_3 & r_1 \end{bmatrix} = \begin{bmatrix} B+\mathrm{j}C & (D+\mathrm{j}E)/b \\ b(-E+\mathrm{j}D) & B+\mathrm{j}C \end{bmatrix} \tag{6}$$

$$B = \cosh c\cos c$$
$$C = \sinh c\sin c$$
$$D = (\cosh c\sin c + \sinh c\cos c)(1/\sqrt{2})$$
$$E = (\cosh c\sin c - \sinh c\cos c)(1/\sqrt{2})$$

The surface resistance is given by

$$R_{\mathrm{si}} = \begin{bmatrix} 1 & -1/h_{\mathrm{i}} \\ 0 & 1 \end{bmatrix} \quad R_{\mathrm{so}} = \begin{bmatrix} 1 & -1/h_{\mathrm{o}} \\ 0 & 1 \end{bmatrix} \tag{7}$$

$$\begin{bmatrix} T_{\mathrm{i}} \\ q_{\mathrm{i}} \end{bmatrix} = \begin{bmatrix} 1 & -(1/h_{\mathrm{i}}) \\ 0 & 1 \end{bmatrix} \begin{bmatrix} r_1 & r_2 \\ r_3 & r_1 \end{bmatrix} \begin{bmatrix} 1 & -(1/h_{\mathrm{o}}) \\ 0 & 1 \end{bmatrix} \begin{bmatrix} T_{\mathrm{o}} \\ q_{\mathrm{o}} \end{bmatrix} \tag{8}$$

$$\begin{bmatrix} T_{\mathrm{i}} \\ q_{\mathrm{i}} \end{bmatrix} = \begin{bmatrix} A_1 & A_2 \\ A_3 & A_1 \end{bmatrix} \begin{bmatrix} T_{\mathrm{o}} \\ q_{\mathrm{o}} \end{bmatrix} \tag{9}$$

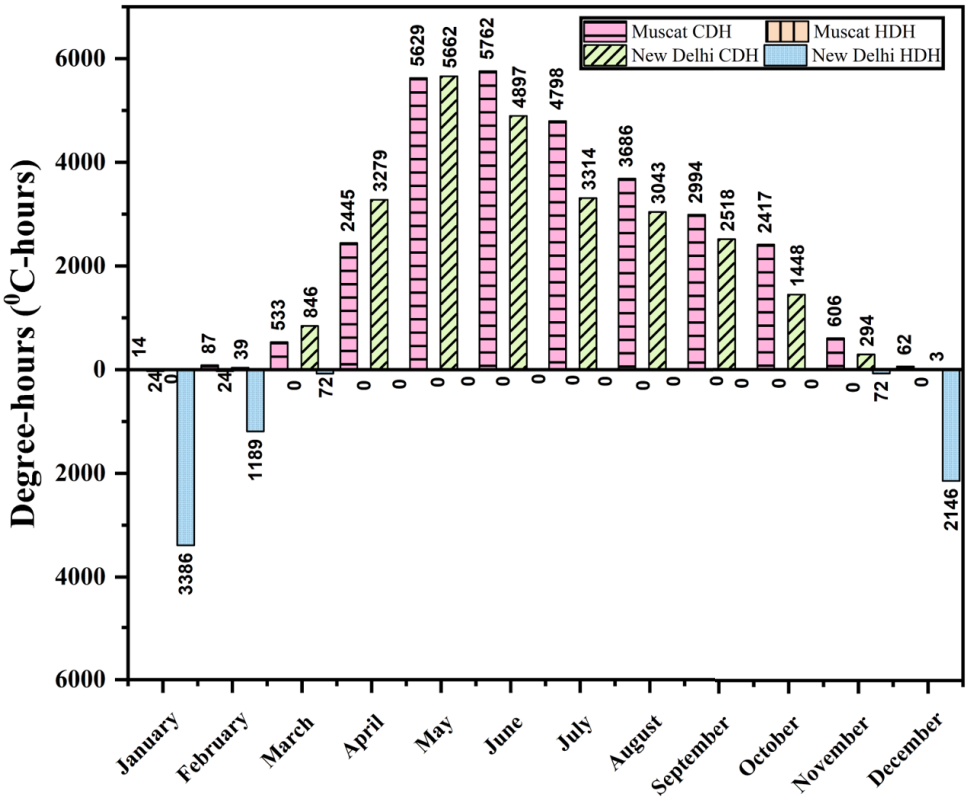

Figure 3. Monthly degree-hours for cooling and heating of Muscat and New Delhi.

Unsteady thermal transmittance (U) considers both thermal mass and thermal insulation components. It can be mathematically calculated using Equation (10):

$$U = \left| -\frac{1}{A_2} \right| \tag{10}$$

A MATLAB program has been formulated and subsequently verified by conducting a thorough assessment using the information provided in the CIBSE guidelines [33]. The convective heat transfer coefficient for the external surface (h_o) is determined to be 25 W·m^{-2}·K^{-1}, whereas the convective heat transfer coefficients for the internal surfaces (h_i) are established as 7.7 and 10 W·m^{-2}·K^{-1} for walls and roofs, respectively, in accordance with the guidelines set forth by the CIBSE (2006).

2.3. *Energy-economic analysis*

Heating degree-hours (HDH) and cooling degree-hours (CDH) serve as essential metrics for quantifying the annual energy requirements for heating and cooling operations, respectively. In the context of thermal engineering, the performance of mechanical systems is fundamentally tied to a base temperature that maintains thermal comfort within the boundaries of a structure. The sol-air temperature is the temperature that gives the combined effect of outdoor temperature distribution and incident solar radiation. Energy-economic analyses are utilized to obtain key metrics such as payback times, carbon emission reductions, and savings in air conditioning costs [34,35]. The monthly degree-hours for Muscat (23.6086 °N, 58.9754 °E) and New Delhi (28.57 °N, 77.12 °E) are also documented in this study.

The HDH and CDH can be calculated using Equations (11) and (12), respectively:

$$\mathrm{HDH} = \sum_{1}^{\mathrm{HD}} (T_b - T_s) = N_{\mathrm{HD}} \Delta T \tag{11}$$

$$\mathrm{CDH} = \sum_{1}^{\mathrm{CD}} (T_s - T_b) = N_{\mathrm{CD}} \Delta T \tag{12}$$

Here, N_{HD} and N_{CD} represent the number of heating and cooling hours, respectively. According to

ASHRAE standards, the minimum base temperatures (T_b) of 18 °C and 23.3 °C for the winter (HDH) and summer (CDH) months have been considered, respectively.

Heating cost savings (HCS) and cooling cost savings (CCS) collectively constitute the overall A/C cost reduction (C_s). The cost of electricity (C_{el}) and the cost of natural gas (C_{ng}) have been considered as per the local rates in New Delhi and Muscat.

For New Delhi, C_{el} = 0.082 \$/kWh and C_{ng} = 0.014 \$/kWh.

For Muscat, C_{el} = 0.026 \$/kWh and C_{ng} = 0.01 \$/kWh.

$$\mathrm{HCS} = \frac{0.001 \cdot \Delta U \cdot \mathrm{HDH} \cdot C_{ng}}{\eta} \tag{13}$$

$$\mathrm{CCS} = \frac{0.001 \cdot \Delta U \cdot \mathrm{CDH} \cdot C_{el}}{\mathrm{COP}} \tag{14}$$

ΔU = change in transmittance
C_{el} = cost of electricity (\$/kWh)
C_{ng} = cost of natural gas (\$/kWh).

The amount of time needed to recover the cost of the original building supplies is referred to as the payback period. Equation (15) shows the relation between total A/C cost reduction and the insulation cost.

$$\mathrm{PBP} = \frac{C_i}{C_s} \tag{15}$$

where C_i is the insulating material cost (\$/kg) and C_s is the air conditioning cost reduction (\$).

Yearly carbon reduction, which is calculated using Equations (16) and (17), represents the total amount of carbon reduction caused by heating and cooling energy savings (COP = 2.5, η = 0.8).

$$\mathrm{HCM} = \frac{0.001 \cdot \Delta U \cdot \mathrm{HDH} \cdot m_c}{\mathrm{COP}} \tag{16}$$

$$\mathrm{CCM} = \frac{0.001 \cdot \Delta U \cdot \mathrm{CDH} \cdot m_n}{\eta} \tag{17}$$

m_c: amount of CO_2 released for each unit of electricity (kg/kWh)
m_n: amount of CO_2 released for each unit of natural gas (kg/kWh).

2.4. *Experimental methodology*

After the completion of water curing and air-drying procedures, a series of tests were conducted on both the standard and the 12 modified concrete samples. The primary focus was on evaluating the thermophysical attributes and compressive strength of these samples. A compression testing machine, conforming to IS 516 standards, was utilized for this assessment. The thermophysical properties, including thermal conductivity and specific heat, were measured using the hot wire probe technique via a KD2 Pro device (Figure 4). Two holes, each 1.3 mm in diameter and 30 mm in length, were drilled to accommodate probes specifically designed for measuring these attributes. The thermophysical properties of the tested materials are summarized in Table 3. Thermal conductivities of the modified concrete samples were measured at room temperature, as shown in Figure 4. The measurements were conducted using the KD2 Pro thermal property analyzer, which offers a precision range of ±5 to ±10% for thermal conductivity and ±10% for specific heat.

2.5. *Measurement of compressive strength*

Compressive strength tests were conducted on specimens containing varying proportions of plastic materials. These tests were performed using a digital compression testing machine that conforms to IS 14858, as shown in Figure 5(a). Following the testing procedures outlined in IS 516 [36], both conventional concrete samples and those containing plastic additives were evaluated. The assessment revealed that conventional concrete exhibits a compressive strength of 36.1 MPa, which serves as a benchmark for comparing the plastic-admixed samples. The inclusion of plastic materials generally led to a reduction in compressive strength, with values ranging from 12.4 to 34.2 MPa depending on the type and proportion of plastic used.

The failure pattern of cubes of different mixes after the compression test can be classified as non-explosive failure. Such a pattern of failure satisfied the failure modes in accordance with BS EN 12390-3. Through visual inspection, it can also be seen that most of the cube specimens showed the cracking to be at approximately 45° to the axis near the ends.

3. Results and discussion

In this section, we present a detailed analysis of the outcomes from the experimental investigations into concrete samples modified with recycled plastics.

Figure 4. Evaluation of thermal properties using the KD2 Pro thermal property analyzer.

Table 3. Thermophysical properties of materials

S. No	Material	K (W·m^{-1}·K^{-1})	C_p (J·kg^{-1}·K^{-1})	ρ (kg/m^3)	Compressive strength (MPa)
1	Low-density polyethylene 10%	0.568 ± 0.002	1096.79 ± 3	2126.2 ± 2	18.36 ± 0.01
2	Low-density polyethylene 20%	0.523 ± 0.003	1227.47 ± 5	2031 ± 4	16.21 ± 0.04
3	Low-density polyethylene 30%	0.48 ± 0.002	1474.37 ± 4	1943.2 ± 3	12.4 ± 0.02
4	Polypropylene 10%	0.956 ± 0.005	881.97 ± 3	2330 ± 4	26.35 ± 0.01
5	Polypropylene 20%	0.823 ± 0.004	1034.12 ± 4	2110 ± 5	22.54 ± 0.02
6	Polypropylene 30%	0.712 ± 0.002	1070.50 ± 3	2085 ± 2	21.88 ± 0.03
7	High-density polyethylene 10%	0.612 ± 0.005	1106.16 ± 5	2336 ± 4	22.46 ± 0.02
8	High-density polyethylene 20%	0.584 ± 0.004	1281.18 ± 4	2201.1 ± 3	18.35 ± 0.01
9	High-density polyethylene 30%	0.592 ± 0.003	1331.81 ± 2	2185 ± 2	14.12 ± 0.04
10	Polyester 10%	0.991 ± 0.005	942.02 ± 5	2349.2 ± 5	34.2 ± 0.05
11	Polyester 20%	0.949 ± 0.004	985.96 ± 3	2422 ± 3	32.1 ± 0.03
12	Polyester 30%	0.931 ± 0.005	1045.63 ± 5	2458.8 ± 2	28.6 ± 0.04
13	Conventional concrete	1.42 ± 0.003	1126 ± 6	2482 ± 6	36.1 ± 0.02

The discussion explores the impacts of these modifications on the mechanical and thermophysical properties of concrete, as well as the economic and environmental implications of their use in sustainable construction. Initially, the morphological characteristics of the modified concrete are examined to understand the microstructural changes imparted by the inclusion of plastic additives. This analysis is critical for interpreting the variations in compressive strength and thermal conductivity observed. Subsequent discussions focus on assessing the potential benefits in terms of energy efficiency, specifically through reductions in air conditioning costs and carbon emissions. These results are contextualized within the broader framework of advancing sustainable building practices.

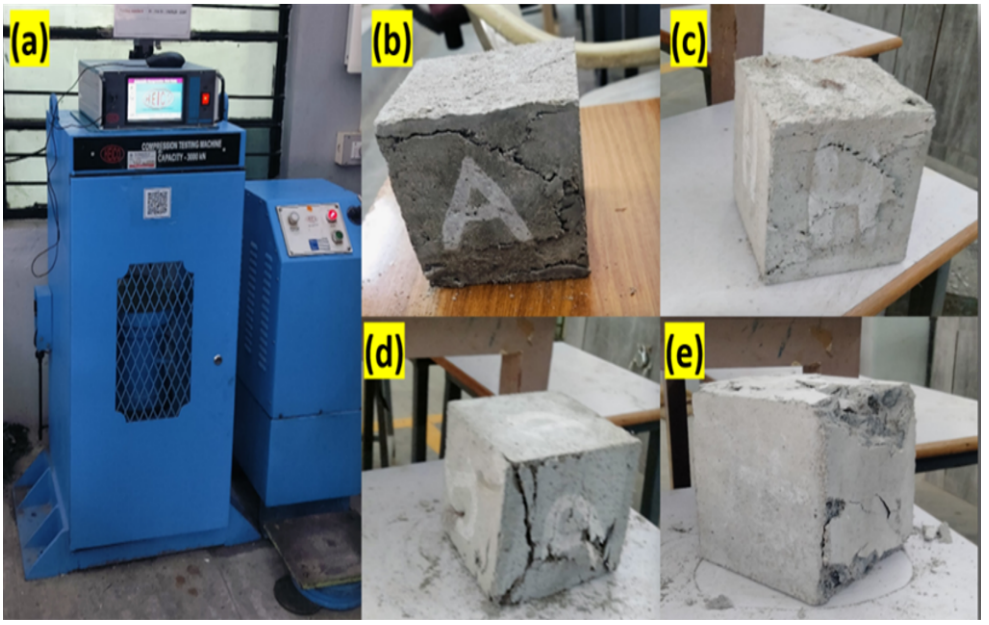

Figure 5. (a) Digital compression testing machine, (b) low-density polyethylene, (c) polypropylene, (d) high-density polyethylene, and (e) polyester.

3.1. *Scanning electron microscope*

The morphological characteristics of the concrete with various plastic admixtures were scrutinized utilizing scanning electron microscope (SEM) images at differing magnification levels as shown in Figure 6. The added admixtures, ranging in size from 0.7 to 0.9 mm, were predominantly uniformly distributed throughout the concrete specimen. The SEM images revealed that these plastic admixtures formed a seamless layer within the concrete matrix, a phenomenon consistently observed across all samples. Consequently, it can be concluded that the incorporation of plastic admixtures did not exert a detrimental impact on the morphological properties of the concrete. The morphologies of the admixture-based concrete samples and conventional concrete seem to be similar when observed under an SEM. The reduction in compressive strength of the samples having more admixture content is attributed to the variation in density when compared to conventional concrete.

3.2. *Yearly A/C cost savings*

The total air conditioning cost savings are derived from reductions in both heating and cooling expenses. These savings have been achieved by incorporating various types of waste plastics into concrete roof structures. To assess the efficacy of these modifications, the air conditioning costs for roofs made with the modified concrete are compared against those for conventional concrete roofs. Figure 7 illustrates the annual savings in air conditioning costs for two distinct climatic zones: Muscat, characterized by a hot and dry climate, and New Delhi, which experiences a composite climate. Among all the range of modified concrete samples studied, the concrete roof containing 30 wt% LDPE exhibited the highest annual air conditioning cost savings, registering values of 0.9946 \$/m^2 for Muscat and 0.9928 \$/m^2 for New Delhi, respectively.

3.3. *Annual carbon emission mitigation*

Figure 8 exhibits the yearly reduction in carbon emissions achieved by different admixture-based concrete roofs, assessed in two separate climate regions, namely Muscat and New Delhi. The annual mitigation of carbon emissions represents the overall reduction, stemming from combined savings in cooling and heating energy. This includes reduced electricity and natural gas consumption, resulting in

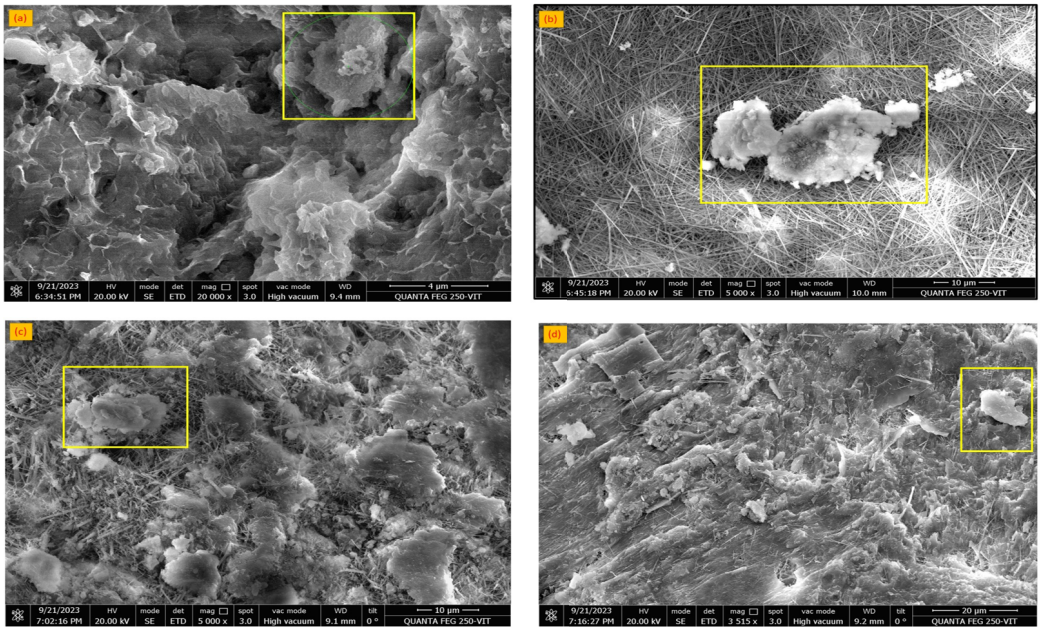

Figure 6. SEM images of various admixture-based concrete samples with 10 wt% of sand replaced by: (a) LDPE, (b) polypropylene, (c) HDPE, and (d) polyester.

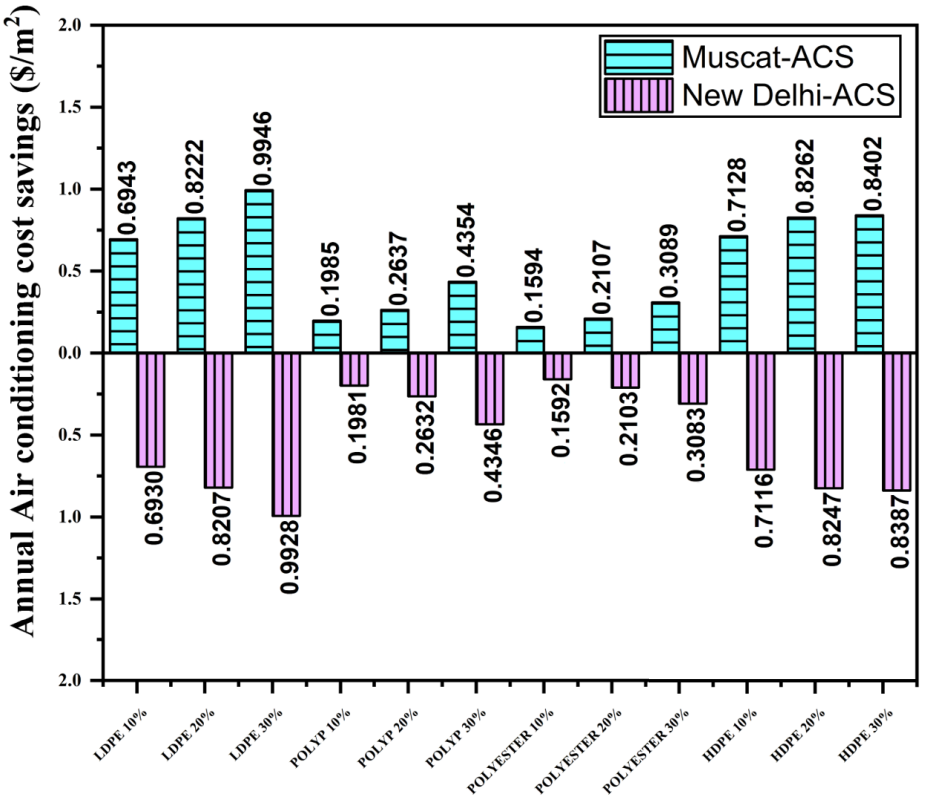

Figure 7. Annual air conditioning cost savings ($/m^2).

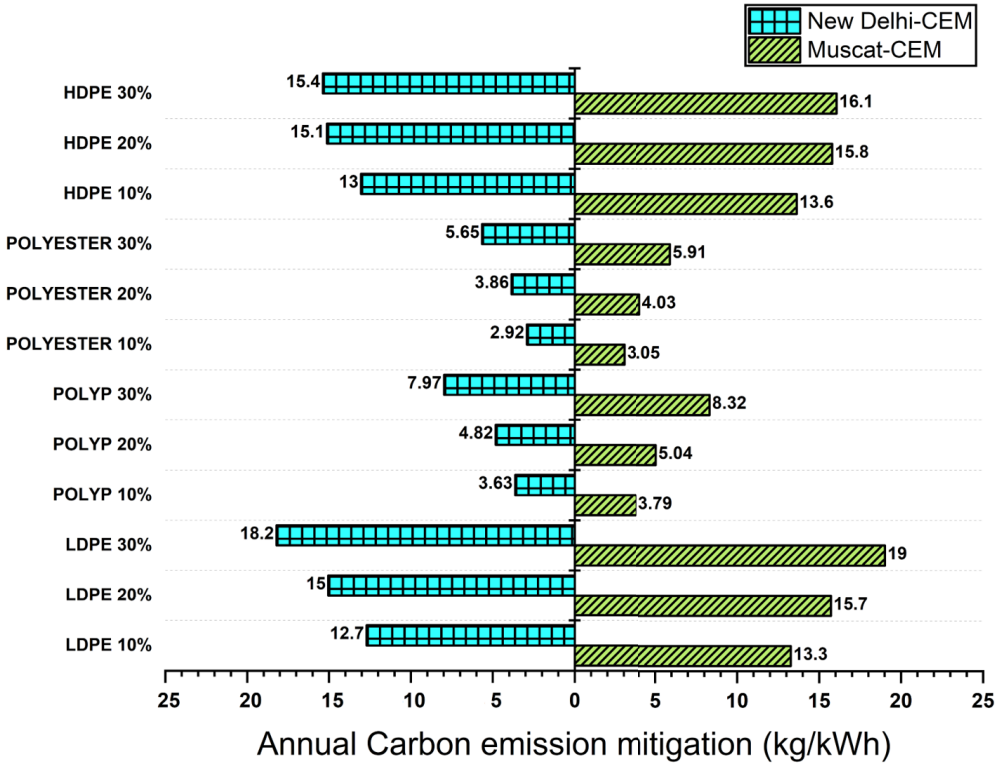

Figure 8. Annual carbon emission mitigation (kg/kWh).

the total carbon emission mitigation measured in kg/kWh. A modified concrete roof that yields higher air conditioning savings also results in greater carbon emission mitigation, thus affirming its environmental sustainability. For the climate of Muscat, the addition of 10 wt% polyester or PP shows a reduction in carbon emissions of 3.05 kg/kWh and 3.79 kg/kWh, respectively. Likewise, the inclusion of 30 wt% LDPE shows the highest carbon emission reduction, measured at 19 kg/kWh. In the climatic conditions of New Delhi, roofs with 10 wt% PP and polyester result in carbon emission reductions of 3.63 kg/kWh and 2.92 kg/kWh, respectively. Moreover, 30 wt% LDPE shows the highest carbon emission reduction, recorded at 18.2 kg/kWh.

3.4. *Payback period*

Figure 9 illustrates the PBPs associated with different admixture-based concrete roofs, showing shorter durations for composite climates such as New Delhi compared to Muscat's hot and dry conditions. In Muscat, the roofs incorporating varying ratios of LDPE, PP, polyester, and HDPE exhibited PBPs of 3.14, 5.3, 6.57, 7.33, 11.30, 10.32, 6.54, 9.9, 10.13, 1.36, 2.35, and 3.47 years, respectively. Remarkably, the roof with 10 wt% HDPE showed the shortest PBP of 1.37 years. Similarly, in the composite climate of New Delhi, roofs with different proportions of LDPE, PP, polyester, and HDPE had PBPs of 3.14, 5.32, 6.58, 7.34, 11.32, 10.33, 6.55, 9.92, 10.15, 1.37, 2.37, and 3.49 years, respectively. Again, the roof with 10 wt% HDPE displayed the shortest PBP, measured at 1.37 years. These observations underscore that the hierarchy of energy efficiency remains consistent, irrespective of the specific climatic conditions.

3.5. *Compressive strength*

Figure 10 shows the mean compressive strength of the modified concrete specimens compared to the conventional block specimens. Conventional concrete has a mean compressive strength of 36.1 MPa. It is observed that the addition of LDPE, PP,

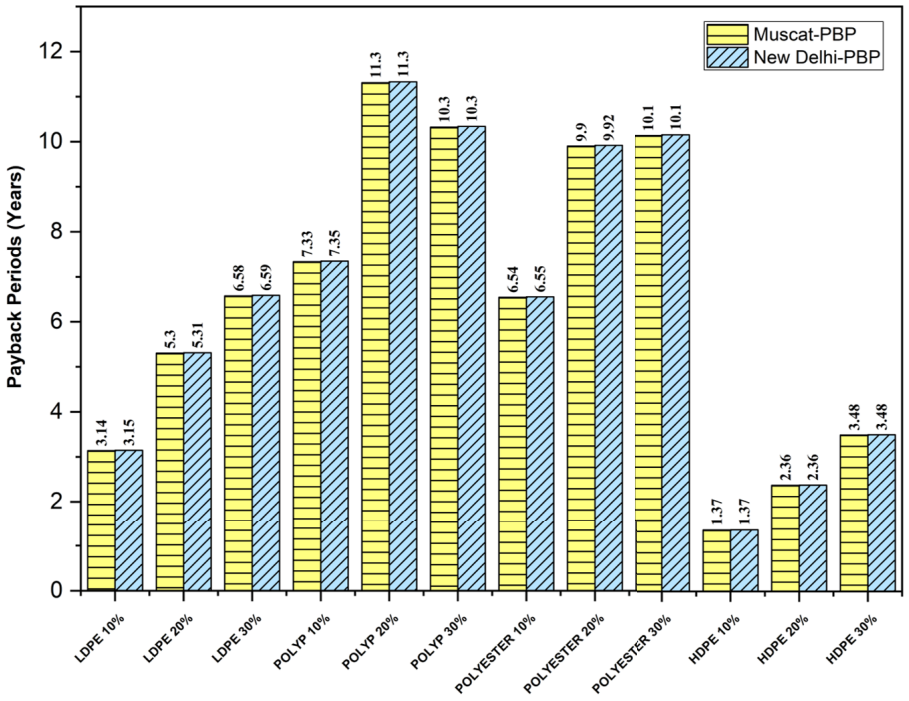

Figure 9. Payback period (years).

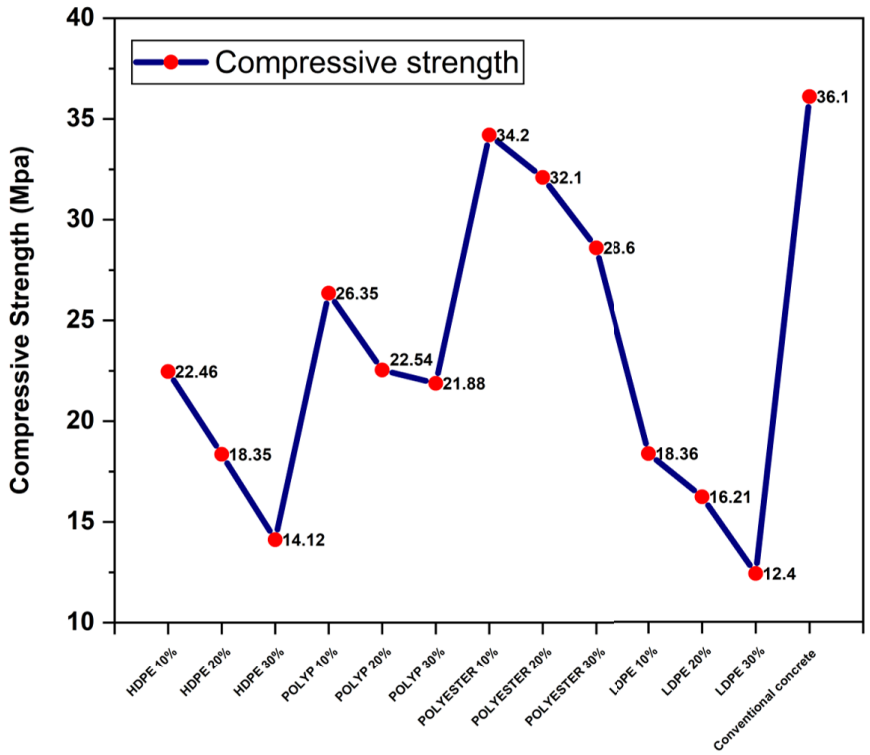

Figure 10. Compressive strength of the modified concrete samples compared with conventional concrete.

polyester, and HDPE as a percentage of sand replacement results in a decline in compressive strength. However, with the addition of 10 wt% polyester, the compressive strength is nearly equal to that of conventional concrete.

In our analysis, it was observed that the inclusion of 30 wt% LDPE led to the most significant decrease in compressive strength. This phenomenon can be attributed to the inherent properties of LDPE, which has a lower density (915 kg/m^3) compared to traditional sand and aggregate materials. The substitution of a significant proportion of these heavier materials with lighter LDPE results in a lower overall density of the concrete mix, which consequently leads to reduced compressive strength. For reference, the densities of other plastics used were as follows: polyester at 1500 kg/m^3, PP at 930 kg/m^3, and HDPE at 925 kg/m^3. The varying densities of these materials correlate with their differing impacts on the structural integrity of the concrete.

4. Conclusion

This study conducted a comprehensive thermoeconomic assessment of concrete specimens that incorporated four distinct types of recycled plastic materials—LDPE, PP, polyester, and HDPE. It was found that these materials, when used as partial substitutes for sand, significantly enhanced the thermal performance of the concrete compared to conventional samples. The assessments were performed under the specific climatic conditions of Muscat and New Delhi, showcasing regional adaptability. The research explored various impacts of using plastic in concrete, focusing on mechanical properties and environmental implications. It was observed that incorporating plastics influenced the compressive strength and density of the concrete blocks.

In summary, the following key observations were made based on the research conducted:

- Among all the modified concrete samples incorporating LDPE in various wt%, it was found that 30 wt% LDPE yielded the most substantial annual savings in air conditioning costs. Specifically, the cost savings were calculated to be $0.9946 per square meter for Muscat and $0.9928 per square meter for New Delhi.
- The analysis of the annual carbon emission mitigation indicates that the samples with a 30 wt% LDPE composition exhibited the most remarkable reduction. The values were quantified as 19 kg/kWh for Muscat and 18.2 kg/kWh for New Delhi.
- The PBP for each of the concrete samples was evaluated, revealing that HDPE added at a 10 wt% replacement level for sand had the shortest payback duration, amounting to 1.37 years for both the Muscat and New Delhi climate conditions.
- It was empirically determined that the incorporation of LDPE, PP, polyester, and HDPE as a percentage of sand replacement in the concrete samples led to a reduction in compressive strength.
- Remarkably, the addition of 10 wt% polyester to the concrete mixture yielded a compressive strength almost equivalent to that of conventional concrete.

These observations serve to underline the potential for incorporating specific types of plastic waste materials as partial sand replacements in concrete mixes to achieve both environmental sustainability and economic viability.

5. Limitations and future research

5.1. *Limitations*

This study highlights the potential of plastic-infused concrete for sustainable construction but recognizes several limitations. The scalability of production and the economic feasibility of implementing such materials on a larger scale were not explored. Additionally, the environmental impacts, including toxicity and potential leaching effects of the plastics used, were not thoroughly examined. Assessments of the thermal stability of materials under various climatic conditions were also absent, which are critical for validating their use in diverse environments.

5.2. *Future research*

Future studies should expand the scope by exploring additional types of waste plastics and conducting long-term performance evaluations under different

environmental conditions. It is also crucial to investigate the environmental safety of these materials, particularly focusing on their toxicity and leaching potential. Further research should aim to validate the mechanical and thermal properties of plastic-infused concrete across varied climatic conditions to enhance its application in sustainable building practices.

Nomenclature

A_1, A_2, A_3	Variables showing input and output heat flow (-)
b	Slab admittance ($W \cdot m^{-2} \cdot K^{-1}$)
c	Cyclic thickness (m)
C_{el}	Cost of electricity ($/kWh)
C_i	Insulating material cost ($/kg)
C_{ng}	Cost of natural gas ($/kWh)
C_p	Specific heat capacity ($kJ \cdot kg^{-1} \cdot K^{-1}$)
C_s	Air conditioning cost reduction ($)
h_i	Convective heat transfer coefficients for internal surfaces ($W \cdot m^{-2} \cdot K^{-1}$)
h_o	Convective heat transfer coefficient for the external surface ($W \cdot m^{-2} \cdot K^{-1}$)
K	Thermal conductivity ($W \cdot m^{-1} \cdot K^{-1}$)
l	Finite thickness (m)
M	Heat flux (W/m^2)
m_c	Amount of CO_2 released for each unit of electricity (kg/kWh)
m_n	Amount of CO_2 released for each unit of natural gas (kg/kWh)
N	Thermal resistance ($m^2 \cdot K/W$)
N_{CD}	Number of cooling hours (h)
N_{HD}	Number of heating hours (h)
p	period (s)
q	Periodic heat flux (W/m^2)
r_1, r_2, r_3, r_4	Specific construction material (-)
R_{si}	Internal surface resistance ($m^2 \cdot K$)/W
R_{so}	External surface resistance ($m^2 \cdot K$)/W
s	Time span (s)
T	Periodic temperature (°C)
T_b	Base temperature (°C)
T_i	Indoor temperature (°C)
T_m	Mean daily temperature (°C)
U	Unsteady thermal transmittance use (kg/kWh)
V	Building material thickness (m)
T_∞	Outdoor air temperature (°C)

Greek letters

α	Thermal diffusivity (m^2/s)
ΔU	Change in transmittance ($W \cdot m^{-2} \cdot K^{-1}$)
η	Efficiency of natural gas power generation for heating (-)
ρ	Density (kg/m^3)
τ	Time variable (h)

Acronyms

CCM	yearly carbon reduction by cooling (kg/kWh)
CCS	cooling cost savings ($/m^2)
CDH	cooling degree-hours (°C-h)
COP	coefficient of performance (-)
HCM	yearly carbon reduction by heating (kg/kWh)
HDH	heating degree-hours (°C-h)
HDPE	high-density polyethylene
HCS	heating cost savings ($/m^2)
LDPE	low-density polyethylene
PBP	payback period (years)
PP	polypropylene

Declaration of interests

The authors do not work for, advise, own shares in, or receive funds from any organization that could benefit from this article, and have declared no affiliations other than their research organizations.

References

[1] F. I. Aneke, B. Awuzie, *Acta Structilia*, 2018, **25**, 119-137.
[2] H. T. Mohan, K. Jayanarayanan, K. M. Mini, *Eng. Sci. Technol. Int. J.*, 2022, **32**, article no. 101060.
[3] P. O. Awoyera, A. Adesina, *Case Stud. Constr. Mater.*, 2020, **12**, article no. e00330.
[4] R. Kumar, M. Kumar, I. Kumar, D. Srivastava, *Mater. Today Proc.*, 2021, **46**, 6775-6780.
[5] D. Muheise-Araalia, S. Pavia, *Constr. Build. Mater.*, 2021, **268**, article no. 121118.
[6] Z. Bashir, M. Amjad, S. F. Raza, S. Ahmad, M. Abdollahian, M. Farooq, *Sustainability (Switzerland)*, 2023, **15**, article no. 8291.
[7] F. Tahir, S. Sbahieh, S. G. Al-Ghamdi, *Mater. Today Proc.*, 2022, **62**, 4013-4017.
[8] J. O. Akinyele, U. T. Igba, T. O. Ayorinde, P. O. Jimoh, *Case Stud. Constr. Mater.*, 2020, **13**, article no. e00404.

[9] P. Kulkarni, V. Ravekar, P. Rama Rao, S. Waigokar, S. Hingankar, *Clean. Mater.*, 2022, **5**, article no. 100113.
[10] B. Balasubramanian, G. V. T. Gopala Krishna, V. Saraswathy, K. Srinivasan, *Constr. Build. Mater.*, 2021, **278**, article no. 122400.
[11] P. Muthupriya, B. VigneshKumar, V. K. Shankar, *Mater. Today Proc.*, 2023 (in press).
[12] C. Arumugam, S. Shaik, A. H. Shaik, K. J. Kontoleon, D. Mazzeo, B. Pirouz, *J. Build. Eng.*, 2022, **45**, article no. 103495.
[13] I. Almeshal, B. A. Tayeh, R. Alyousef, H. Alabduljabbar, A. M. Mohamed, *J. Mater. Res. Technol.*, 2020, **9**, 4631-4643.
[14] S. Pratap Singh Rajawat, B. Singh Rajput, G. Jain, *Mater. Today Proc.*, 2022, **62**, 6824-6831.
[15] P. Janardhan, H. Narayana, N. Darshan, *Mater. Today Proc.*, 2023 (in press).
[16] S. Vivek, P. Hari Krishna, T. D. Gunneswara Rao, *Mater. Today Proc.*, 2023 (in press).
[17] D. C. Ali, A. K. Jassim, R. Al-Sabur, *J. Sustain. Dev. Energy Water Environ. Syst.*, 2023, **11**, 1-13.
[18] M. Idrees, A. Akbar, F. Saeed, M. Gull, S. M. Eldin, *Alexandria Eng. J.*, 2023, **68**, 405-416.
[19] S. Arya, R. Sharma, R. Rautela, S. Kumar, *Sustain. Energy Technol. Assess.*, 2023, **57**, article no. 103253.
[20] T. Saravanan, G. Durga Devi, *Mater. Today Proc.*, 2023 (in press).
[21] M. S. Haque, *Environ. Sci. Pollut. Res.*, 2019, **26**, 36163-36183.
[22] S. Shaik, A. Roy, M. Arıcı, K. J. Kontoleon, A. Afzal, D. Li, *Energy Build.*, 2023, **286**, article no. 112955.
[23] A. B. Puttaranga, S. Talanki, S. Saboor, A. Babu, T. Puttaranga Setty, S. Shaik, *International High Performance Buildings Conference*, 2016, Paper 197. Available: http://docs.lib.purdue.edu/ihpbc/197.
[24] C. Arumugam, S. Shaik, *Environ. Sci. Pollut. Res.*, 2021, **28**, 15259-15273.
[25] Y. Luan, Y. Ma, T. Ma, C. Wang, F. Xia, *Constr. Build. Mater.*, 2023, **400**, article no. 132773.
[26] S. Maqbool, A. H. Khan, M. A. Rizvi, A. Inam, F. A. Kashmiri, *Ain Shams Eng. J.*, 2022, **13**, article no. 101512.
[27] J. P. Zachariah, P. P. Sarkar, M. Pal, *Constr. Build. Mater.*, 2021, **269**, article no. 121357.
[28] C. Arumugam, S. Shaik, *Sustain. Energy Technol. Assess.*, 2021, **48**, article no. 101657.
[29] ASHRAE, *Int. J. Refr.*, 1979, **2**, 56-57.
[30] J. A. Duffie, W. A. Beckman, J. McGowan, *Am. J. Phys.*, 1985, **53**, 382-382.
[31] S. Shaik, A. B. Talanki Puttaranga Setty, *Build. Environ.*, 2016, **99**, 170-183.
[32] S. Shaik, A. B. P. S. Talanki, *Environ. Sci. Pollut. Res.*, 2016, **23**, 9334-9344.
[33] CIBSE, *CIBSE Environmental Design Guide A*, The Chartered Institution of Building Services Engineers, London, 2006.
[34] A. Chel, G. N. Tiwari, *Appl. Energy*, 2009, **86**, 1956-1969.
[35] S. Saboor, K. K. G, V. Kumar, K.-H. Kim, T. P. Ashok Babu, *Energy Build.*, 2018, **173**, 326-336.
[36] B. of Indian Standards, *IS 516: Part 1: Sec 1: 2021: Hardened concrete methods of test, Part 1: Testing of strength of hardened concrete, Section 1: Compressive, flexural and split tensile strength (First Revision)*, Bureau of Indian Standards, New Delhi, 2021.